Tel1 activation by the MRX complex is sufficient for telomere length regulation but not for the DNA damage response in *S. cerevisiae*

Rebecca Keener*†, Carla J. Connelly*, Carol W. Greider*

*Department of Molecular Biology and Genetics, Johns Hopkins University School of Medicine, Baltimore, Maryland 21205 †Biochemistry, Cellular and Molecular Biology Graduate Program, Johns Hopkins University School of Medicine, Baltimore, Maryland 21205.

Running Title: Pathways for telomeres and repair

Keywords: Tel1, MRX complex, telomere, DNA damage response, epistasis

Corresponding Author: Carol W. Greider

Address: 725 N. Wolfe St. PCTB 603 Baltimore, Maryland 21205

Phone Number: 410-955-3292

e-mail address: cgreider@jhmi.edu

Abstract

Previous models suggested that regulation of telomere length in *S. cerevisiae* by Tel1(ATM) and Mec1(ATR) parallel the established pathways regulating the DNA damage response. Here we provide evidence that telomere length regulation differs from the DNA damage response in both the Tel1 and Mec1 pathways. We found that Rad53 mediates a Mec1 telomere length regulation pathway but is dispensable for Tel1 telomere length regulation, whereas in the DNA damage response Rad53 is regulated by both Mec1 and Tel1. Using epistasis analysis with a Tel1 hypermorphic allele, Tel1-hy909, we found that the MRX complex is not required downstream of Tel1 for telomere elongation but is required downstream of Tel1 for the DNA damage response. Since models that invoke a required end processing event for telomerase elongation are primarily based on the yeast pathways, our data call for a re-examination of the requirement for telomere end processing in both yeast and mammalian cells.

Introduction

Telomere length regulation is critical for cell viability and disruption of length homeostasis leads to disease (STANLEY AND ARMANIOS 2015). Telomerase adds telomere repeats onto chromosome ends and redundant pathways tightly regulate this addition. In humans, decreased telomerase activity causes short telomere syndromes (ARMANIOS AND BLACKBURN 2012) while telomerase activation promotes cancer growth (GREIDER 1999). Thus, understanding the feedback pathways for maintaining telomeres is critical to understanding disease. The Ataxia Telangiectasia-Mutated (ATM) and Ataxia-Telangiectasia and Rad3-related (ATR) checkpoint kinases play a role in both sensing damage and maintaining telomeres around an equilibrium point in yeast (RITCHIE *et al.* 1999) and in mammalian cells (LEE *et al.* 2015; TONG *et al.* 2015; DE LANGE 2018) yet their underlying mechanisms remain unclear.

In *Saccharomyces cerevisiae* multiple independent pathways control telomere length. Tel1, the ATM homolog, and Mec1, the ATR homolog, regulate partially redundant pathways that affect both telomere length and the DNA damage response. *TEL1* and *MEC1* mutations shorten telomeres, although *TEL1* deletion has a greater effect on telomere shortening than *MEC1* mutants. However, the double mutant has an additive effect on telomere shortening, suggesting the kinases regulate parallel pathways (RITCHIE *et al.* 1999). While hypomorphs in *MEC1* show clear telomere shortening, *MEC1* deletions have led to some conflicting conclusions in the literature (DI DOMENICO *et al.* 2014). *MEC1* is an essential gene as *mec1Δ* cells are inviable because they are not able to activate dNTP production. *mec1Δ* cells survive only with co-

89 deletion of either *SML1* or *CRT1*, and in *mec1Δ sml1Δ* or *mec1Δ crt1Δ* cells, dNTP production is
90 increased. *mec1Δ sml1Δ* and *mec1Δ crt1Δ* have different effects on telomere length which has
91 been attributed to the fact that *SML1* and *CRT1* regulate different pathways of dNTP production
92 (MAICHER *et al.* 2017). Mec1 and Tel1 also both play a role in the DNA damage response, where
93 Mec1 has the greater effect. *TEL1* deletion on its own does not show DNA damage sensitivity,
94 but strains with mutations in both *TEL1* and *MEC1* show higher sensitivity to DNA damage than
95 *MEC1* mutation alone (MORROW *et al.* 1995). These experiments indicate that *TEL1* and *MEC1*
96 have roles in both the DNA damage response and telomere length regulation.
97
98 The distinct effects of *tel1Δ* and *mec1Δ* on telomere length and the DNA damage response
99 suggest Tel1 and Mec1 may have different critical substrates. Both Tel1 and Mec1
100 phosphorylate S/T-Q motifs (KIM *et al.* 1999). This identical phosphorylation motif has made
101 identifying unique substrates of each kinase challenging. Mass spectrometry approaches have
102 identified specific Tel1 and Mec1 substrates, in addition to shared substrates (BASTOS DE OLIVEIRA
103 *et al.* 2015), but the biological consequences of these phosphorylation events remain unclear.
104
105 While hundreds of Tel1/Mec1 substrates have been identified, those that are critical for the
106 DNA damage response and telomere length have not been defined. We investigated the role of
107 two known substrates: Rad53 and the MRX complex. Both candidates were reported to be
108 phosphorylated by Tel1 and/or Mec1 in response to DNA damage (D'AMOURS AND JACKSON 2001;
109 NAKADA *et al.* 2003b; SMOLKA *et al.* 2007; ALBUQUERQUE *et al.* 2008; BASTOS DE OLIVEIRA *et al.* 2015;
110 LAVIN *et al.* 2015). In the DNA damage response, both Tel1 and Mec1 phosphorylate Rad53,

activating it's kinase activity (Figure 1A)(NAKADA *et al.* 2003b). However, Tel1 phosphorylation is considered less important relative to Mec1 phosphorylation of Rad53 (USUI *et al.* 2001). In response to a double-strand break, Tel1 interaction with the MRX complex activates Tel1 kinase activity and Tel1 subsequently phosphorylates the MRX complex, in addition to other substrates (LEE *et al.* 2013; BASTOS DE OLIVEIRA *et al.* 2015). The MRX complex resects the double-strand break to facilitate repair and several studies indicate that Tel1 modulates this process (LAVIN *et al.* 2015). In this model the MRX complex can be considered both upstream and downstream of Tel1 for the DNA damage response (Figure 1A). Several studies have suggested that similar regulatory events occur at the telomere (TSUKAMOTO *et al.* 2001; LARRIVEE *et al.* 2004; VISCARDI *et al.* 2007; BONETTI *et al.* 2009), although specific mechanisms are not well established.

In this study we used mutagenesis and epistasis analysis to show that *RAD53* is in the *MEC1* telomere length pathway. In addition, epistasis analysis showed the MRX complex acts both upstream and downstream of Tel1 in the DNA damage response, as characterized by others. However, strikingly, the MRX complex is only required upstream of Tel1 in telomere length regulation. Therefore, while the MRX complex is required to activate Tel1 kinase activity, it is not required for telomere resection. These findings demonstrate that the regulation of these proteins in the DNA damage response are distinct from their regulation in telomere length maintenance and challenge the assumption that a telomere must be resected by the MRX complex for telomere elongation by telomerase.

Materials and Methods

Molecular Cloning

Each plasmid was constructed using Gibson Assembly (GIBSON 2011), for detailed explanations of cloning strategies see File S1. Primers were designed using Snapgene software (GSL Biotech), products were amplified with Phusion HS II DNA polymerase (Thermo Fisher F549), and Gibson Assembly Master Mix (New England Biolabs E5510) was used according to the New England Biolabs (NEB) recommended protocol. All restriction enzymes and NEB5α competent cells (NEB C2987H) are from NEB. Plasmids were prepared using QIAprep Miniprep Kit (Qiagen 27106) and all sequencing was performed using the Sanger method.

Site-directed mutagenesis

S/T-Q mutations and *TEL1-hy909* mutations were introduced by site-directed mutagenesis using primers designed by PrimerX.org. Primer sequences are listed in Table S3. In each case, the plasmid was amplified using PfuTurbo (Agilent 600252). The product was *Dpn*I-treated, ethanol precipitated, and transformed into DH5α cells (Thermo Fisher 18265017). Clones were isolated and sequence verified.

Yeast culturing and transformation

Yeast culturing, transformation, and sporulation were conducted as described in (GREEN AND SAMBROOK 2012). Briefly, transformation was carried out on 50 mL of logarithmically cultured cells treated with 0.1 M Lithium Acetate (LiAc, Sigma L6883). DNA was added to a 50 µL aliquot of cells in addition to 50 µg boiled fish sperm carrier DNA (Roche 11467140001). Cells were equilibrated at 30° for 10 minutes after which 0.5 mL 40% Polyethylene glycol (PEG_{4000}, Sigma P4338) containing 0.1 M LiAc was added. Cells were incubated at 30° for 30 minutes then heat shocked at 42° for 15 minutes. Transformed cells were washed with sterile water and plated on the appropriate selective media. In cases where an antibiotic selectable marker was used, cells were recovered in 1 mL Yeast-extract Peptone Dextrose (YPD) at 30° for 3-4 hours before plating. One-step integration was used for all integrated constructs. After transformation, integration at the desired locus was confirmed by junction Polymerase Chain Reaction (PCR). In cases where mutations were introduced, the region was amplified using Phusion HS II DNA polymerase the amplicon was purified using AMPure beads (Beckman Coulter A63881), and sequenced to confirm the presence of mutations *in vivo*.

Passaging yeast

Because we initiate our experiments with strains that are heterozygous for multiple alleles of interest, dissection of twenty tetrads often yields all combinations of the alleles. This makes it possible to obtain experimental and control samples in parallel. Treating all haploids in parallel is critical for evaluating telomere length as telomere length can be sensitive to differences in culturing time. In cases where the diploid genotype did not allow isolation of an important

control, a second diploid, from which that control can be segregated, was dissected in parallel. After tetrad dissection and replica plating to identify segregants of interest, haploids were streaked to single cell on a YPD plate. This streak was designated as the first passage, after which these cells are estimated to have undergone 40 population doublings. Subsequently, cells were re-streaked repeatedly to increase the number of cell divisions. Each passaged plate was incubated for 48 hours at 30° after which cells were picked from the streak dilution and re-streaked to single cell again on a fresh plate. Each passage is estimated to require approximately 20 population doublings. Therefore, a strain passaged five times undergoes a total of approximately 120 population doublings. At the desired number of passages, cells were inoculated into a 5 mL liquid YPD culture and grown at 30° overnight or until saturated. Cell pellets were saved at -20° until all time points had been collected, at which time genomic DNA was extracted. Images of the plates at specific time points were taken to document potential growth defects.

MRX-tag and _mrx-18A_ strain construction

A yRK1006 *MRE11-3HA-URA3* segregant was mated to a yRK2040 *RAD50-G6-V5-LEU2* segregant, yielding yRK1. The *XRS2-13myc-hphMX4* construct (pRK1028) was transformed into yRK1, yielding yRK60. A yRK60 segregant with all three *MRX-tag* components was mated to a *mec1Δ sml1Δ* haploid (JHUy816 segregant) to yield yRK79 and yRK80. The *mrx-18A* parental diploids were constructed in a manner parallel to the *MRX-tag* parental diploids. A yRK1052 *mre11-4A-3HA-URA3* segregant was mated to a yRK2082 *rad50-10A-G6-V5-TRP1* segregant,

yielding yRK26. The *xrs2-4A-13myc-hphMX4* construct (pRK1040) was transformed into yRK26, yielding yRK56. A yRK56 segregant with all three *mrx-18A* components was mated to a *mec1Δ sml1Δ* haploid (yYM242 segregant) to yield yRK81 and yRK83. Mutations were confirmed again in yRK81 and yRK83 by sequencing.

rad50S knock-in using CRISPR/Cas9

gRNA sequences were chosen using the algorithms published by Doench et al. via the Benchling (Biology Software, 2019) interface (DOENCH *et al.* 2016). Two guides, RW 670 and RW 671, were individually cloned into pCAS026 using the strategy described by Anand et al. (ANAND *et al.* 2017). gRNA sequences are listed in Table S3. Double-stranded homology repair templates were amplified (primers RW 674, RW 675) using a 90-mer oligonucleotide as the template. The repair template was designed to both introduce the Rad50S mutation (Lys81Ile) (ALANI *et al.* 1990) and introduce a silent mutation in the Protospacer Adjacent Motif (PAM) sequence. Primer RW 672 was used as the template for the RW 670 guide and primer RW 673 was used as the template for the RW 671 guide. SPRI beads (Beckman Coulter B23318) were used to purify the repair template before transformation. yRK114 haploid cells were cultured for transformation as described above except that no carrier DNA was added and 100 µL of cells were used in the transformation reaction. Cells were transformed with 1 µg of pCAS026 containing the appropriate guide and 4-5 µg of double-stranded repair template. Cells were grown on minimal media without uracil to select for cells that contained the pCAS026 plasmid. The *rad50S* allele was validated by sequencing. yRK2112 was edited using the RW 670 guide

while yRK2116 was edited using the RW 671 guide. yRK2113 was transformed with pCAS026 containing the RW 670 guide but was not edited and was used in parallel to serve as a control. Haploids were streaked on minimal media containing 5-Fluoroorotic Acid (5-FOA) (Toronto Research Chemicals F595000) to select against the pCAS026 plasmid followed by five passages on YPD plates before telomere elongation was observed by Southern blot (data not shown).

Southern blot analysis

Genomic DNA was extracted and used for Southern blot analysis as described previously (KAIZER *et al.* 2015). Briefly, a cell pellet of approximately 50 µL was resuspended in 1x Lysis Buffer (10 mM Tris, pH 8.0, 0.5 M EDTA, pH 8.0, 100 mM NaCl, 1% SDS, 2% Triton X-100) and cells were lysed in the presence of 0.3mm glass beads (Biospec products, Inc. 11079105). Phenol-chloroform (50:50) was added and cells were vortexed for 8 min (Eppendorf mixer 5432). The DNA was ethanol precipitated and resuspended in 40-50 µL TE (10 mM Tris, pH 8.0, 1 mM EDTA) with RNaseA (10 µg/mL) at 37° for one hour or 4° overnight.

Samples were cut with the restriction enzyme *Xho*I and electrophoresed at 47 V (12 mA) on a 1.0% agarose in 1x TTE buffer (20x = 1.78 M Tris base, 0.57 M Taurine, 0.01 M EDTA) for approximately 24 hours. 200 ng of 2-log DNA ladder (NEB N3200) was included for reference. The genomic DNA was transferred to a Hybond N+ membrane (GE Healthcare RPN303B) by vacuum blotting (Boekel Appligene vacuum blotter) for 1 hour at 50 mbar with the gel covered in 10x SSC buffer (1.5 M NaCl, 0.17 M sodium citrate). Once transferred, the DNA was UV

crosslinked (Stratagene UV Stratalinker 2400). The membrane was prehybridized in Church buffer (0.5 M Tris, pH 7.2, 7% SDS, 1% bovine serum albumin, 1 mM EDTA) at 65° then α^{32}P-dCTP-radiolabeled (Perkin Elmer) fragments of the Y' element and the 2-log DNA ladder were added at 10^6 cpm/mL and 10^4 cpm/mL, respectively. The membrane was incubated with the radiolabeled probe overnight, washed in 1x SSC, 0.1% SDS buffer at 65°, imaged with a Storage Phospho Screen (GE Healthcare) overnight and then scanned on a Storm 825 imager (GE Healthcare). The images were copied from ImageQuant (GE Life Sciences) to Adobe PhotoShop CS6 and saved as .tif files. The images were cropped in Adobe PhotoShop CS6 to show only the telomere restriction fragment.

Western blot

Protein extracts were prepared by Trichloroacetic acid (TCA) extraction (LINK AND LABAER 2011). Samples were resolved on a NuPAGE 3-8% Tris-Acetate gradient polyacrylamide gel (Invitrogen EA0375) in 1x Tris-Acetate running buffer (Invitrogen LA0041) using the Invitrogen NuPAGE system with protein ladder standards (Bio-Rad 161-0374). The gel was transferred by electroblotting to a PVDF membrane (Thermo Fisher IPFL00010) using NuPAGE transfer buffer (20x: 40.8 g Bicine, 52.4 g Bis-Tris, 3.0 g EDTA) at 30 V for 1.5 hours. The membrane was blocked with Odyssey buffer (Li-Cor 927-40000) for 1 hour at room temperature or overnight at 4°. Primary antibodies were diluted in blocking buffer and incubated at room temperature for 1 hour (Sigma Aldrich M2 Flag at 1:1,000; Invitrogen 22C5D8 Pgk1 at 1:6,000; Roche 12CA5 HA at 1:2,000; Invitrogen R960-25 V5 at 1:2,000; Santa Cruz 9E10 c-myc at 1:10,000). The membrane

was washed in 1x Tris Buffered Saline with Tween-20 (TBST) buffer (10x TBST: 0.2 M Tris Base, 1.5 M NaCl, 1% Tween-20) before incubation at room temperature for 30 minutes with a Horse Radish Peroxidase (HRP) conjugated secondary antibody (Bio-Rad 1706516 at 1:10,000) in 5% powdered milk (Bio-Rad 170-6404) resuspended in 1x TBST. The membrane was washed in 1x TBST and then incubated with Forte HRP substrate (Millipore WBLUF0100) followed by imaging on ImageQuant LAS 4000 mini biomolecular imager (GE Healthcare). The images were copied from ImageQuant (GE Life Sciences) to Adobe PhotoShop CS6 and saved as .tif files.

Mutagen challenge

Strains of interest were inoculated to an initial OD600 of 0.15-0.25 in 8-10 mL YPD. Once the density reached an OD600 of 0.5-0.6, the culture was split into untreated and treated samples. 4-nitroquinoline (Sigma N8141) was resuspended in acetone at a stock concentration of 1 mM. 15U Bleomycin (Fresenius Kabi C103610) was dissolved in 10 mL sterile water and used as a 1 mg/mL stock. Hydroxyurea (US Biologicals H9120) was resuspended in sterile water at a stock concentration of 1 M. Methyl methanesulfonate (MMS) (Sigma 129925) was treated as 100%. The appropriate chemical was added to each treated sample and cultured at 30° with slight agitation for 1-2 hours, as indicated in the figure legends. Untreated samples were cultured in parallel. Cell pellets of equal density were collected for each sample based on the OD600. The size of the cell pellet varied between experiments from 0.6 OD to 8.0 OD, as indicated in the figure legends. Each pellet was resuspended in 1 mL YPD and serially diluted 1:5 in YPD in a 96-well dish. 4 µL of each dilution was spotted onto a YPD plate and the plates were cultured at

30° for 48 hours before being imaged on a Bio-Rad Gel Doc XR+ Imaging System under white light using Image Lab 6.0.1 software.

Quantitative MMS survival assay

Freshly grown strains of interest were inoculated to an initial OD600 of 0.2-0.3 in 6 mL YPD. Once density reached 0.5-0.6 OD600, an untreated sample was plated for each strain before cells were treated with 0.01% MMS. 30-minute time points were taken up to 120 minutes for each strain. A Millipore Scepter with 40 µm tips was used to measure cells/mL at each time point. Approximately 500 cells were plated across five YPD plates, with approximately 100 cells per plate, for each strain and at each timepoint. Samples were blinded before plating and the plates were incubated at 30° for 48 hours. Colony forming units were counted for each blinded sample and once all plates were counted, the results were unblinded. At each timepoint the number of colonies was calculated as a proportion: the total number of colonies for that strain at that timepoint relative to the total number of colonies for that strain at the untreated time point (t=0). Data were graphed using Prism 5.0b and the standard error of the mean is shown.

Plasmid end-joining assay

Cells were cultured and treated as described above for yeast transformation. Once density reached an OD600 of 0.6-0.8 the cells were transformed with 100 ng of *Stu*I-linearized pRS317 (SIKORSKI AND BOEKE 1991), which generates blunt ends, or with 100 ng of circular pRS317. 50 µg

boiled fish sperm carrier DNA (Roche 11467140001) was added to both linear and circular transformation reactions. Three replicate transformations were performed for both linear and circular plasmids and for each strain. Cells were plated on minimal media without lysine. After 48 hours of incubation at 30°, colony forming units were counted. The average number of colonies of the three replicates containing circular DNA was calculated for each strain. Each linear DNA transformation was treated as a technical replicate. The number of colonies from each linear DNA transformation plate was normalized to the average number of colonies of circular DNA for that strain. Data were plotted and analyzed in Prism 5.0b. An unpaired two-tailed student *t*-test was performed between samples.

Data Availability Statement

All strains and plasmids are available upon request. The Reagent Table provides a reference for all genes, strains, software, and many reagents used in this study. Table S1 contains all strains used in this study. Table S2 contains all plasmids used in this study and a brief description of their purpose. Table S3 contains all primers used in this study and a brief description of their purpose. File S1 has a detailed explanation of how all plasmids used in this study were constructed. All supplemental files, including the Reagent Table, have been uploaded to fig**share**.

Results

Rad53 regulates telomere length through the Mec1 pathway

Rad53 kinase is a candidate substrate that could mediate telomere length since both Tel1 and Mec1 phosphorylate Rad53 and kinase-dead Rad53 has short telomeres (LONGHESE *et al.* 2000; NAKADA *et al.* 2003b). We used epistasis and mutational analyses to examine whether Rad53 functions in the Tel1 or Mec1 telomere length pathway (Figure 1A). We deleted either *SML1* or *CRT1,* regulators of dNTP pools that were previously shown to suppress the lethality of *mec1Δ* and *rad53Δ (HUANG et al. 1998; ZHAO et al. 1998)*. While it is most common in the literature to use *sml1Δ* to rescue *mec1Δ* lethality*,* there is evidence that *SML1* deletion can mask telomere length phenotypes (LONGHESE *et al.* 2000). Therefore, we initially compared the effects of deleting *sml1Δ* or *crt1Δ* on telomere length in *tel1Δ* or *mec1Δ* mutants.

All of our experiments were carried out in haploid yeast, however, to avoid telomere length changes that can occur with long term propagation of haploids, we standardly generated fresh haploids by sporulating heterozygous diploids (see methods). We generated diploid strains that were heterozygous for *TEL1/tel1Δ MEC1/mec1Δ SML1/sml1Δ* and *CRT1/crt1Δ* and then sporulated to obtain haploids with specific mutant combinations. While *sml1Δ* and *mec1Δ sml1Δ* cells had telomeres similar to wild-type cells, *crt1Δ* cells had slightly shorter telomeres (Figure 1B, compare lanes 2-5 to lanes 6-7) and *mec1Δ crt1Δ* cells had shorter telomeres than *crt1Δ* cells (Figure 1B, compare lanes 8-9 to lanes 6-7). *mec1Δ crt1Δ* telomeres were similar to

353 the short telomeres reported in *mec1-1* and *mec1-21* cells (data not shown)(RITCHIE *et al.* 1999).
354 *tel1Δ sml1Δ* cells showed short telomeres very similar to *tel1Δ* mutants. However, *tel1Δ crt1Δ*
355 telomere lengths were slightly shorter than *tel1Δ sml1Δ* (Figure 1B, compare lanes 14-15 to
356 lanes 16-17). We conclude that *sml1Δ* masks the short telomere phenotype of *mec1Δ* cells
357 while *crt1Δ* does not, although *crt1Δ* has a mild telomere shortening effect on its own.
358
359 To examine whether Rad53 plays a role in the Tel1 or Mec1 telomere length pathway, we
360 generated diploids heterozygous for *TEL1/tel1Δ MEC1/mec1Δ RAD53/rad53Δ* and *CRT1/crt1Δ*
361 and sporulated to obtain specific mutant combinations. We observed that *crt1Δ* suppresses
362 *rad53Δ* lethality, consistent with previous reports (Figure S1B) (HUANG *et al.* 1998). We
363 compared *mec1Δ crt1Δ* telomeres to *mec1Δ rad53Δ crt1Δ* and observed no additive shortening
364 (Figure 1C, compare lanes 7-8 to lanes 5-6), which is consistent with Rad53 functioning in the
365 Mec1 telomere length regulation pathway. In contrast, we found there was additive shortening
366 in *tel1Δ rad53Δ crt1Δ* telomeres compared to *tel1Δ crt1Δ* (Figure 1C, compare lanes 11-12 to
367 lanes 15-16), supporting the conclusion that Tel1 and Rad53 are in different length regulation
368 pathways. However, *tel1Δ rad53Δ crt1Δ* telomeres were slightly longer than *tel1Δ mec1Δ crt1Δ*
369 telomeres (Figure 1C, compare lanes 11-12 to lanes 13-14), suggesting that either Rad53 has
370 functions in both the Tel1 and Mec1 telomere length pathways or that Rad53 acts exclusively in
371 the Mec1 telomere length pathway which also relies on additional Mec1 substrates for
372 telomere length regulation.
373
374 **Phosphorylation of Rad53 on S/T-Q motifs regulates telomere length**

375

376 To examine the role of Rad53 as a Tel1/Mec1 substrate that mediates telomere length, we
377 examined a Rad53 mutant where Tel1/Mec1 S/T-Q phosphorylation motifs were mutated to A-
378 Q. Previous work demonstrated that a subset of the Rad53 S/T-Q motif clusters are critical for
379 Rad53 function in the DNA damage response and that this mutant, *rad53*$^{1\text{-}4/9\text{-}12AQ}$, could not
380 respond to Mec1 or Tel1 regulation (Lee *et al.* 2003). Both Rad53 and *rad53*$^{1\text{-}4/9\text{-}12AQ}$ were viable
381 when expressed off of a plasmid using the endogenous promoter in *rad53Δ* cells and did not
382 require co-deletion of *SML1* or *CRT1* (Figure S1A and data not shown). We integrated 3xFLAG-
383 tagged *rad53*$^{1\text{-}4/9\text{-}12AQ}$ or 3xFLAG-tagged *RAD53* at the endogenous locus in *TEL1/tel1Δ*
384 *MEC1/mec1Δ CRT1/crt1Δ* diploid cells to better control the segregation of these alleles. Rad53
385 and Rad53$^{1\text{-}4/9\text{-}12AQ}$ were stably expressed, as shown previously (Lee *et al.* 2003)(data not
386 shown). Unlike the plasmid expression system, we noted that integrated *rad53*$^{1\text{-}4/9\text{-}12AQ}$ is lethal
387 unless it co-segregates with *sml1Δ* or *crt1Δ* (Figure S1B). *rad53*$^{1\text{-}4/9\text{-}12AQ}$ *crt1Δ* cells had shorter
388 telomeres than *RAD53-tag crt1Δ* cells (Figure 1D, compare lanes 7-8 to lanes 5-6),
389 demonstrating that phosphorylation of Rad53 contributes to telomere length regulation.
390
391 We did not observe additive shortening in *mec1Δ rad53*$^{1\text{-}4/9\text{-}12AQ}$ *crt1Δ* cells compared to *mec1Δ*
392 *crt1Δ* or *rad53*$^{1\text{-}4/9\text{-}12AQ}$ *crt1Δ* cells (Figure 1D, compare lanes 15-16 to lanes 17-18 and lanes 13-
393 14), consistent with Mec1 targeting these phosphorylation sites. In contrast, we observed
394 additive shortening in *tel1Δ rad53*$^{1\text{-}4/9\text{-}12AQ}$ *crt1Δ* cells compared to *rad53*$^{1\text{-}4/9\text{-}12AQ}$ *crt1Δ* cells
395 (Figure 1D, compare lanes 9-10 to lanes 7-8), further supporting the conclusion that Tel1 and
396 Rad53 are in different pathways. We observed only a slight shortening in *tel1Δ rad53*$^{1\text{-}4/9\text{-}12AQ}$

397 *crt1Δ* cells compared to *tel1Δ crt1Δ* cells (Figure 1D, compare lanes 9-10 to lanes 11-12). Similar
398 to our earlier findings, this is consistent with either Tel1 and Mec1 phosphorylate Rad53 for
399 telomere length regulation or that there are other Mec1 substrates that are key for telomere
400 length in addition to Rad53.
401
402 **Tel1-hy909 requires Rad53 for DNA damage response but not for telomere length regulation**
403
404 To directly examine whether Tel1 telomere length regulation is Rad53-dependent, we
405 performed epistasis analysis with *rad53Δ crt1Δ* and a Tel1 hypermorphic allele, *TEL1-hy909,*
406 which has increased Tel1 kinase activity, increased DNA damage response function, and long
407 telomeres (BALDO *et al.* 2008). We generated diploids heterozygous for *TEL1/TEL1-hy909*
408 *RAD53/rad53Δ* and *CRT1/crt1Δ* and diploids heterozygous for *TEL1/TEL1-hy909 MEC1/mec1Δ*
409 and *CRT1/crt1Δ*. We first examined the DNA damage response in haploid cells by challenging
410 them with a DNA-damaging agent, methyl methanesulfonate (MMS). *mec1Δ crt1Δ* cells were
411 sensitive to DNA damage while *TEL1-hy909 mec1Δ crt1Δ* cells were not (Figure 2A), consistent
412 with previous reports (BALDO *et al.* 2008). This indicates that Tel1 hyperactivity can rescue the
413 DNA damage response in a *mec1Δ* mutant. Like *mec1Δ crt1Δ,* the *rad53Δ crt1Δ* cells were also
414 sensitive to DNA damage (Figure 2B). However, unlike *TEL1-hy909 mec1Δ crt1Δ* cells, *TEL1-*
415 *hy909 rad53Δ crt1Δ* cells were still sensitive to MMS challenge (Figure 2B). Further, while *TEL1-*
416 *hy909* was able to rescue *mec1Δ* lethality (Figure S2A), as previously shown (BALDO *et al.* 2008),
417 *TEL1-hy909* was not able to rescue *rad53Δ* lethality (Figure S2B). These data indicate that Rad53
418 is essential to mediate the Tel1-hy909 DNA damage response.

We next examined telomere length in *TEL1-hy909* and *TEL1-hy909 rad53Δ crt1Δ* mutants. *TEL1-hy909 rad53Δ crt1Δ* cells had an intermediate telomere length between *TEL1-hy909* and *rad53Δ crt1Δ* (Figure 2C). This indicates that either Rad53 has a partially redundant role in the Tel1 telomere length regulation pathway or that Rad53 and Tel1 function in independent pathways. We reasoned that if Rad53 was important for Tel1-hy909 telomere elongation then telomeres would not further elongate with increased divisions in the absence of Rad53. We passaged *TEL1-hy909 rad53Δ crt1Δ* cells and observed that telomeres elongated with further passages (Figure 2D). This suggests that Rad53 is not required for Tel1 telomere length regulation which is in stark contrast to the Rad53-dependence of Tel1-hy909 for the DNA damage response (Figure 2A). Together, these data suggest that Rad53, likely with other unidentified proteins, functions in the Mec1 telomere length pathway, but is not required in the Tel1 telomere length pathway.

S/T-Q sites in MRX affect the DNA damage response but not telomere length regulation

Having found that Rad53 is not essential to mediate the Tel1 telomere length response, we next tested whether the MRX complex might be a critical Tel1 substrate. In both yeast and mammalian cells, all three components of the MRX(N) complex are phosphorylated by Tel1/Mec1 (ATM/ATR) (D'AMOURS AND JACKSON 2001; NAKADA *et al.* 2003b; SMOLKA *et al.* 2007; ALBUQUERQUE *et al.* 2008; BASTOS DE OLIVEIRA *et al.* 2015; LAVIN *et al.* 2015). Tel1 and Mec1 have a well characterized and conserved S/T-Q phosphorylation motif (KIM *et al.* 1999). Previous work

showed that mutation of all S/T-Q motifs in Xrs2 to A-Q had no effect on the DNA damage response or on telomere length (MALLORY *et al.* 2003). To further probe whether MRX phosphorylation affects function, we mutated all S/T-Q motifs across the entire MRX complex and examined the effect on DNA damage response and telomere length.

Each MRX gene was epitope-tagged, the S/T-Qs were mutated to A-Qs, and the construct was integrated at the endogenous locus (Figure 3A). We generated three strains with each gene individually mutated at all S/T-Q sites, termed *mre11-4A*, *rad50-10A*, and *xrs2-4A*, as well as a strain containing all three mutants, termed *mrx-18A* (see methods). As a control, we generated a strain with all three proteins epitope-tagged but with wild-type coding sequence, referred to as *MRX-tag*. Individually, and in combination with one another, the altered proteins were stable as determined by western blot, indicating that mutations do not affect protein stability (Figure 3B).

To examine the role of Tel1 and Mec1 phosphorylation of MRX on the DNA damage response, we tested the *mrx-18A* mutant for MMS sensitivity. None of the MRX S/T-Q mutants individually or in combination showed increased sensitivity to MMS, hydroxyurea, bleomycin, or 4-nitroquinoline (Figure S3A and data not shown). We noted *tel1Δ* alone does not have detectable MMS sensitivity (Figure S3A) but there is an observable increase in MMS sensitivity in *tel1Δ mec1Δ sml1Δ* compared to *mec1Δ sml1Δ* (Figure S3B). To take advantage of this increased sensitivity, we put *mrx-18A* and *MRX-tag* in the sensitized background of *mec1Δ sml1Δ* and assayed cells for an increased MMS sensitivity compared to *mec1Δ sml1Δ* alone.

463

464 Using the spotting assay, it was difficult the determine whether the sensitivity of *mrx-18A*
465 *mec1Δ sml1Δ* cells was increased compared to *MRX-tag mec1Δ sml1*Δ cells (Figure S3B). To
466 quantify the subtle DNA damage defect of *mrx-18A mec1Δ sml1Δ* cells we used a more sensitive
467 assay where colony forming units are counted as cells are treated with MMS over time. In this
468 quantitative assay we observed no difference in MMS sensitivity between *mrx-18A mec1Δ*
469 *sml1Δ* cells compared to *MRX-tag mec1Δ sml1*Δ (Figure 3C). We also noted in this assay that
470 *MRX-tag mec1Δ sml1Δ* cells were slightly more sensitive than *mec1Δ sml1Δ*, suggesting the tags
471 have a small effect on MRX complex function (Figure 3C). The epitope tags do not greatly
472 disrupt function as this small effect was only observed in a *mec1Δ sml1*Δ sensitized background.
473 No increased sensitivity was observed in response to 4-nitroquinoline, bleomycin, or
474 hydroxyurea (Figure S4A-C). As a control, we also examined *mrx-18A tel1Δ,* and found no
475 increased MMS-sensitivity (Figure S4D).

476

477 In addition to its role in homology-directed repair, MRX also plays a critical role in Non-
478 Homologous End Joining (NHEJ) in yeast (MOORE AND HABER 1996). We tested the effect of *mrx-*
479 *18A* on NHEJ using a plasmid re-ligation assay (BOULTON AND JACKSON 1996) and found no effect
480 of *mrx-18A* compared to *MRX-tag* (Figure 3D). These data suggest that phosphorylation of MRX
481 by on S/T-Q sites does not play a major role in NHEJ.

482

483 We next examined the telomere length phenotype of the *mrx-18A* mutant and found no effect
484 compared to the *MRX-tag* cells. *MRX-tag* cells exhibited slight telomere shortening compared

485 to untagged alleles, consistent with a slight defect seen in the DNA damage assay, however,
486 *mre11Δ* was significantly shorter by comparison (Figure 3E). Individual mutant subunits, *mre11-*
487 *4A, rad50-10A, and xrs2-4A,* also had no effect on telomere length (Figure S5). To determine
488 whether a change in telomere length would be seen after further cell divisions, we streaked
489 *mrx-18A* cells for approximately 120 population doublings and still saw no effect on telomere
490 length (Figure 3F). These data suggest that phosphorylation of the MRX complex by Tel1 or
491 Mec1 on S/T-Q sites is not critical for telomere length regulation.
492
493 **MRX is required downstream of Tel1 for the DNA damage response but not telomere length**
494
495 The lack of requirement for MRX phosphorylation by Tel1 or Mec1 raised the question of
496 whether MRX is required downstream of Tel1. Because double mutants of either *mre11Δ,*
497 *rad50Δ, or xrs2Δ* with *tel1Δ* produces a short telomere phenotype similar to any individual
498 mutant, it is not possible to establish epistasis. Therefore, we performed epistasis analysis with
499 the *TEL1-hy909* hypermorphic allele and *mre11Δ, rad50Δ, or xrs2Δ*. As described earlier, *TEL1-*
500 *hy909* elongates telomeres and provides a stark contrast to the short telomeres in *mre11Δ,*
501 *rad50Δ, or xrs2Δ* cells. Many studies suggest Tel1 and MRX act in the same epistasis pathway
502 and current models indicate that MRX recruits Tel1 to a DNA double-strand break, activates the
503 kinase, Tel1 phosphorylates MRX, and then MRX processes DNA ends for repair (OH AND
504 SYMINGTON 2018; PAULL 2018). Analogous pathways have been proposed for Tel1 and MRX in
505 telomere length regulation, (TSUKAMOTO *et al.* 2001; VISCARDI *et al.* 2007; BONETTI *et al.* 2009)

506 predicting that the MRX complex is downstream of Tel1 and that the MRX complex should be
507 epistatic to Tel1 in both the DNA damage response and telomere length regulation.
508
509 To examine the epistasis of MRX and Tel1, we generated strains heterozygous for *TEL1/TEL1-*
510 *hy909 MEC1/mec1Δ* and *SML1/sml1Δ* together with individual heterozygous deletions of
511 *mre11Δ, rad50Δ, or xrs2Δ* and initially examined the DNA damage response. We observed the
512 *TEL1-hy909 mre11Δ* double mutants were as sensitive to MMS as *mre11Δ* alone (Figure 4A),
513 consistent with previous work (BALDO *et al.* 2008). The other two double mutants, *TEL1-hy909*
514 *rad50Δ* and *TEL1-hy909 xrs2Δ*, were also both MMS sensitive (not shown). These results
515 support a role for MRX downstream of Tel1 in the DNA damage response, as previously
516 reported (MOORE AND HABER 1996; USUI *et al.* 2001). We found that, surprisingly, *TEL1-hy909*
517 *mec1Δ mre11Δ* spores were inviable, indicating the rescue of *mec1Δ* lethality by *TEL1-hy909* is
518 MRX-dependent (Figure S6). This was also true for *TEL1-hy909 mec1Δ rad50Δ* and *TEL1-hy909*
519 *mec1Δ xrs2Δ* (not shown).
520
521 We next examined telomere length in *TEL1-hy909 mre11Δ, TEL1-hy909 rad50Δ,* and *TEL1-hy909*
522 *xrs2Δ* double mutants and found that, surprisingly, in all three cases the double mutants had
523 long telomeres, similar to *TEL1-hy909* alone (Figure 4B). This indicates that, unlike the DNA
524 damage response, MRX is not epistatic to Tel1 for telomere length. Because this result differs
525 from previous findings, we repeated the experiment in the strain background (W303) used in
526 the previous study (BALDO *et al.* 2008). In this analysis, all three independently derived double
527 mutants *TEL1-hy909 mre11Δ, TEL1-hy909 rad50Δ,* and *TEL1-hy909 xrs2Δ* showed long

telomeres consistent with our initial findings (Figure S7A). We also passaged *TEL1-hy909 xrs2Δ* for 120 population doublings to see if shortening might occur with further divisions. Instead, we found telomeres elongated further with passaging (Figure S7B). These data suggest that MRX is not required downstream of Tel1-hy909 to carry out telomere elongation.

To further investigate the requirement of nuclease activity at the telomere, we tested the epistatic relationship between *TEL1-hy909* and deletion of Sae2(CtIP), which stimulates Mre11 (LENGSFELD *et al.* 2007), or Exo1, which has been suggested to play a role in telomere processing (MOREAU *et al.* 2001). We generated diploid strains that were heterozygous for *TEL1/TEL1-hy909 EXO1/exo1Δ* and diploid strains that were heterozygous for *TEL1/TEL1-hy909 SAE2/sae2Δ*. *TEL1-hy909 exo1Δ* cells and *TEL1-hy909 sae2Δ* cells had long telomeres, similar to *TEL1-hy909* alone (Figure 4C, compare lanes 5-6 to lanes 7-8 and lanes 13-14 to lanes 15-16). These data support the hypothesis that telomere resection by MRX/Sae2 or Exo1 is not required for telomere length maintenance.

Rad50S activates Tel1 for telomere length maintenance

The ability of Tel1-hy909 to generate long telomeres in the absences of MRX suggests that this hypermorph is constitutively active as it does not require activation by MRX. As an independent approach to determine whether MRX is only required upstream of Tel1 in telomere length regulation, we performed the a similar epistasis experiment using *tel1Δ* and a previously identified MRX complex mutant, *rad50S* (ALANI *et al.* 1990). Rad50S produces a long telomere

phenotype which has been attributed to increased Tel1 activation (KIRONMAI AND MUNIYAPPA 1997). *rad50S* mutants are reported to have a sporulation defect (USUI *et al.* 2001), therefore we performed these experiments in haploid cells. We used CRISPR/Cas9 to knock-in the *rad50S* allele at the endogenous *RAD50* locus (Anand et al. 2017). Elongated telomeres were observed after cells were passaged for approximately 120 population doublings (Figure 4D, lanes 3-4). In these haploids, we subsequently introduced a *tel1Δ* or *TEL1-hy909* allele at the *TEL1* locus. As a control, parallel strains were generated where a *mre11Δ* allele was introduced at the *MRE11* locus. Without Mre11, Rad50S should not be able function in the MRX complex and the hypermorph activity will not be observed. *rad50S tel1Δ* double mutants showed short telomeres, similar in length to *tel1Δ* (Figure 4D) indicating *rad50S* does not affect telomere elongation by acting downstream of Tel1. Telomere shortening was also observed in *rad50S mre11Δ* cells, as expected (Figure 4D). These experiments suggest that Tel1 is required for the telomere elongation seen in *rad50S* cells. Further, *rad50S TEL1-hy909* had very long telomeres similar to *TEL1-hy909* (Figure 4E). Our data indicate that MRX activates Tel1 but does not contribute to processing of telomeres to allow telomere length regulation after Tel1 activation. In contrast, the MRX complex is critical downstream of Tel1 for the DNA damage response (Figure 5).

Discussion

Telomere elongation and DNA damage response are regulated through different mechanisms

We found that, in contrast to published models, the MRX complex is not required after Tel1 activation for telomere elongation. Our data suggest a new model for the regulation of telomere length in which Tel1 activation by MRX is sufficient for telomere length regulation but not for the DNA damage response (Figure 5). Previous work has shown that Mec1 and Rad53 play a major role in DNA damage response, while Tel1 plays a minor role acting through Rad53 and the MRX complex. In the DNA damage response, the MRX complex is thought to act both upstream and downstream of Tel1 (Usui *et al.* 2001; Paull 2015). MRX binds to double-strand breaks and interacts with Tel1, activating its kinase activity. Previously, a parallel model for telomere length regulation suggested that MRX recruits and activates Tel1 at the telomere, then MRX processes telomere ends to promote telomerase elongation (Larrivee *et al.* 2004; Bonetti *et al.* 2009). In this model, Mec1 is considered secondary to Tel1 for telomere length regulation and its function was presumed to be redundant. In contrast, we show that Mec1 and Rad53 act in a separate, non-overlapping pathway from Tel1 for telomere length maintenance. Together these data demonstrate that the Tel1 and Mec1 pathways differ significantly for the DNA damage response and telomere length regulation.

Dysregulation of dNTP pools can mask telomere length phenotypes

The role of Mec1 in telomere length regulation has remained poorly understood, in part because of discrepancies in reported telomere length phenotypes. *mec1Δ sml1Δ* telomeres appear similar to wildtype while *mec1Δ crt1Δ* telomeres are shorter than wildtype (Figure 1B). Both *sml1Δ* and *crt1Δ* suppress the lethality of *mec1Δ* through upregulation of different pathways that regulate nucleotide pools (HUANG *et al.* 1998; ZHAO *et al.* 1998). Several studies suggest that the increased telomere length in *mec1Δ sml1Δ* compared to *mec1-1* and *mec1-21* alleles is due to increased telomerase processivity with increased dGTP levels (GUPTA *et al.* 2013). Recent work has suggested that while both mutants increase nucleotide pools, *sml1Δ* and *crt1Δ* have different effects on the specific ratio of dGTP to other dNTPs (MAICHER *et al.* 2017). Because dGTP is limiting for telomerase processivity *in vitro* (GREIDER AND BLACKBURN 1987; HAMMOND AND CECH 1997), it was proposed that an increased dGTP/dNTP ratio would elongate telomeres. (MAICHER *et al.* 2017). However, increased dNTP levels are not sufficient to lengthen telomeres, as *sml1Δ* and *crt1Δ* mutants do not show increased telomere length on their own. Also, *crt1Δ* does not lengthen telomeres in either a *tel1Δ* or *mec1Δ* background (Figure 1B). Therefore, while changes in dNTP pools in *mec1Δ sml1Δ* cells may mask telomere length phenotypes (LONGHESE *et al.* 2000) the data are not consistent with altered telomerase processivity as the mechanism.

Rad53 phosphorylation by Mec1 contributes to telomere length regulation

Previous work has shown that Tel1 or Mec1 phosphorylation of Rad53 is critical for the DNA damage response. Our data demonstrate an additional role for Rad53 phosphorylation in

616 telomere length regulation. This phosphorylation is likely primarily performed by Mec1, as our
617 data indicate that Rad53 is in the Mec1 telomere length pathway and it has previously been
618 shown that Mec1 phosphorylation of Rad53 is predominant in the DNA damage response (USUI
619 *et al.* 2001). We cannot exclude the possibility that Tel1 phosphorylation of Rad53 contributes
620 in a small way to telomere length regulation. However, the *TEL1-hy909* hypermorphic allele
621 showed telomere elongation in the absence of Rad53 (Figure 2D), suggesting that Tel1 does not
622 require Rad53 for telomere length regulation. Our model suggests there are as yet unknown
623 substrates that mediate the Tel1 effect on telomere length (Figure 5).
624
625 **Rad53 is a critical mediator of Mec1 in telomere length regulation**
626
627 The *TEL1-hy909* hypermorphic allele can rescue the lethality of *mec1Δ,* as shown previously
628 (BALDO *et al.* 2008). However, we found that *TEL1-hy909* did not rescue *rad53Δ* lethality. Rad53
629 is a substrate of both Tel1 and Mec1 (SANCHEZ *et al.* 1996; SMOLKA *et al.* 2007). Both *mec1Δ* and
630 *rad53Δ* are thought to be lethal due to an inability to upregulate ribonucleotide reductases for
631 DNA repair. Tel1-hy909 has increased catalytic activity *in vitro* and is able to phosphorylate
632 Rad53 more efficiently than Tel1 (BALDO *et al.* 2008). Tel1-hy909 likely rescues *mec1Δ* lethality
633 because of its increased ability to activate Rad53. Our finding that *TEL1-hy909* cannot rescue
634 *rad53Δ* places Rad53 as the critical mediator of Mec1: Mec1 loss can be compensated for by
635 Tel1-hy909 but this hypermorph cannot compensate for loss of Rad53.
636

637 The *MRX* complex is epistatic to *TEL1-hy909* in the DNA damage response, as *TEL1-hy909*
638 *mre11Δ* was just as sensitive as *mre11Δ* to MMS challenge. This was also true for the other MRX
639 complex components. We unexpectedly found that *TEL1-hy909 mec1Δ mre11Δ* is lethal while
640 *TEL1-hy909 mec1Δ* is viable (Figure S6). It is unclear why the *TEL1-hy909* rescue of *mec1Δ*
641 viability is *MRX*-dependent. Previous models would suggest this is because the MRX complex is
642 required for Tel1 activation. However, our data indicate that the *TEL1-hy909* allele is
643 constitutively active.
644
645 **MRX complex phosphorylation by Tel1/Mec1 on S/T-Q sites is not required for DNA damage**
646 **response, NHEJ, or telomere length regulation**
647
648 Multiple studies have reported that Tel1/Mec1-dependent phosphorylation of the MRX
649 complex occurs in response to DNA damage. Thus, were surprised to find that the mrx-18A
650 mutant did not have a DNA damage phenotype or in NHEJ. The absence of an effect on
651 telomere length was also surprising, and suggests MRX is not the substrate that mediates the
652 Tel1 pathway of telomere length regulation.
653
654 **Telomere elongation can occur in the absence of MRX complex**
655
656 The fact that Tel1-hy909 telomere elongation can occur in the absence of the MRX complex
657 indicates that telomere elongation is possible without telomere end processing by MRX. This
658 epistasis indicates that the Tel1-hy909 hypermorph has bypassed the need to interact with

MRX for its activation, and that the point mutations in the *TEL1-hy909* allele promote constitutive catalytic activity. This finding, combined with the fact that the mrx-18A mutant has no telomere length defect, suggest that Tel1 does not require MRX for telomere length regulation after it is activated. Further, the only known mutants in MRX that decrease telomere length are those that decrease the MRX complex interaction with Tel1. (i.e. Xrs2 C-terminal truncation) (NAKADA *et al.* 2003a; MA AND GREIDER 2009). Similarly, mutants that increase telomere length are thought to hyperactivate Tel1 (i.e. *rad50S* and *TEL1-hy* alleles) (KIRONMAI AND MUNIYAPPA 1997; BALDO *et al.* 2008). MRX mutants that alter the catalytic functions of the complex are required for the DNA damage response but not for telomere length regulation. For example, alleles of Mre11 that lack nuclease function do not show a telomere length phenotype (MOREAU *et al.* 1999; TSUKAMOTO *et al.* 2001) but do inhibit the DNA damage response (BUIS *et al.* 2008). Similarly, deletions of the Mre11 nuclease co-factor, Sae2 (CtIP) alone, or in combination with Exo1 deletion, show no telomere length defects (BONETTI *et al.* 2009). This is consistent with our observation that, like *mre11Δ, TEL1-hy909* elongates telomeres in *sae2Δ* and *exo1Δ* cells (Figure 4C). We conclude that cells with deletions of MRX complex components have short telomeres because of the reduction in Tel1 activation, not because the cell lacks the resection functions.

Our finding that MRX is not required downstream of Tel1 for telomere elongation has important implications for telomere elongation models. Most models suggest that after replication of the telomere the leading strand telomere is processes by a nuclease before telomerase can elongate it. The presumption that leading strand replication leaves a blunt end

681 that requires processing is an assumption that has not been directly tested (LINGNER AND CECH
682 1998; PFEIFFER AND LINGNER 2013). In contrast to those models, our data suggest telomerase can
683 efficiently elongate telomeres without end processing. Tel1(ATM) and the MRX(N) complex are
684 thought to function by similar mechanisms in *S. cerevisiae* and mammalian cells (OH AND
685 SYMINGTON 2018; PAULL 2018). Therefore, the data presented here suggest we should rethink the
686 requirements for telomere resection preceding telomere elongation broadly across all
687 organisms.
688
689 **Author Contributions**
690
691 Study conception: CWG and RK, Methodology: RK and CWG, Investigation and Acquisition of
692 data: RK and CC, Supervision: CWG, Formal analysis and interpretation of data: RK and CWG,
693 Validation: RK and CC, Visualization: RK, Data curation: RK, Funding acquisition: CWG, Drafting
694 of manuscript: RK and CWG, Critical revision: RK, CC, and CWG
695
696 **Acknowledgements**
697
698 We thank Rini Mayangsuri for technical assistance with this work. We thank Brendan Cormack,
699 Geraldine Seydoux, the Greider Lab, and the Armanios Lab for critical reading of the manuscript
700 and helpful discussions. This work was supported by Bloomberg Distinguished Professorship (to
701 CWG) and the Turock Fellowship (to RK).
702

703 **Figure Legends**

704

705 **Figure 1 Rad53 is in the Mec1 telomere length regulation pathway**

706

707 (A) Diagram representing a simplified, current understanding of Tel1/Mec1 pathways in the
708 DNA damage response. (B)-(D) Southern blot analysis of telomeres from segregants with the
709 indicated genotype. Two independent, haploid segregants were assayed for each genotype. (B)
710 Haploid cells were passaged on solid media for approximately 120 population doublings to
711 decrease telomere length heterogeneity. Segregants are from JHUy937-1. (C) Segregants are
712 from yRK6002 and yRK6003. (D) Both Rad53 and Rad53$^{1\text{-}4/9\text{-}12AQ}$ are epitope tagged with a
713 3xFLAG tag. Haploids were passaged for approximately 100 population doublings. Segregants
714 are yRK6008-1, yRK6008-2, yRK6009-1, yRK6009-2, yRK6010-1, yRK6010-2, yRK6011-1,
715 yRK6011-2, yRK6012-1, yRK6012-2, yRK6013-1, yRK6013-2, yRK6014-1, yRK6014-2, yRK6015-1,
716 and yRK6015-2.

717

718 **Figure 2 Tel1-hy909 requires Rad53 for the DNA damage response but not telomere**
719 **elongation**

720

721 (A)-(B) Yeast dilution series of untreated cells or cells cultured in 0.02% MMS for one hour. The
722 genotype is indicated to the left of the panels. (A) Segregants are from yRK5126 and yRK5127.
723 (B) Segregants are from yRK5028 and yRK5059. (C) Southern blot analysis of telomeres from
724 segregants with the indicated genotype. Two independent, haploid segregants were assayed

for each genotype. Because the *TEL1-hy909* hypermorph elongates telomeres in the parental diploid (not shown), we observed increased telomere length heterogeneity across all genotypes in the haploid segregants and observe the wild-type segregant telomeres were longer compared to other Southern blots. Segregants are from yRK5028 and yRK5059. (D) Southern blot analysis of telomeres from segregants with the indicated genotype. Segregants were passaged on solid media for approximately 120 population doublings. Passage number is indicated below the genotype as P1 for the first passage or P5 for the fifth passage. Note that the WT telomeres were longer in the parental diploid due to Tel1-hy909. Segregants are from yRK5028.

Figure 3 The mrx-18A S/T-Q mutant does not affect the DNA damage response, NHEJ, or telomere length

(A) Domain structure of the MRX complex indicating location of S/T-Q motifs. Mre11 has an N-terminal nuclease domain and a DNA binding domain. Rad50 has an N-terminal Walker A domain and a C-terminal Walker B domain in addition to central coiled-coil domains (LEE *et al.* 2013). Xrs2 has a Forkhead association (FHA) domain followed by two BRCA1 domains and there is a conserved region near the C-terminus (SHIMA *et al.* 2005; BECKER *et al.* 2006). The domain sizes are relatively to scale for each protein and are consistent with NCBI annotation (Mre11: BAA02017.1, Rad50: CAA65494, Xrs2: AAA35220.1). The location of each S/T-Q motif is indicated with the involved S or T residue number indicated. (B) Western blots examining stability of tagged MRX protein components individually or in combination. Samples were run

and transferred on duplicate gels simultaneously. The membranes were cut such that each protein could be independently probed. Strains used in western blot are yRK114, yRK106, yRK94, yRK138, yRK139, yRK133, yRK135, yRK102, and yRK90. (C) Proportion of colonies on cells treated with 0.01% MMS over 120 minutes (see methods). Proportion is calculated as the number of colonies at that time point for that genotype relative to the number of colonies for that genotype at t=0. The average and standard error of the mean of six technical replicates is plotted for each genotype with error bars only going upward. Strains included are yRK114, yRK128, yRK104, and yRK92. (D) Plasmid end-joining assay results with three technical replicates for each of two biological replicates. Black circles correspond to the first biological replicate and pink triangles correspond to the second biological replicate. The number of linear DNA transformation colonies for each genotype relative to the average number of circular DNA transformation colonies for that genotype. An unpaired two-tailed student *t*-test was performed between the samples. Comparison of *MRX-tag* to *mrx-18A* had a p-value = 0.0.0680 and was not significant (n.s.). *MRX-tag* was not significantly different from wildtype (data not shown). Comparison of *mrx-18A* to *mre11Δ* had a p-values < 0.0001 (***). Strains included are segregants from yRK79, yRK80, yRK81, yRK83, and yRK5064. (E) Southern blot analysis of telomeres from strains with the indicated genotype. Two independent, haploid segregants were assayed for each genotype. The *mre11Δ* haploids were yRK1018 and yRK1019 and were passaged for approximately 200 population doublings. *WT*, *MRX-tag*, and *mrx-18A* haploids were segregants from yRK79, yRK80, yRK81, and yRK83. (F) Southern blot analysis of telomeres from strains with the indicated genotype. Haploid cells were passaged on solid media for approximately 140 population doublings. Passages 1, 3 and 6 are shown for simplicity. Two

769 independent haploids segregants were assayed for each genotype. There were no growth
770 defects observed over time. Segregants are from JHUy868, yRK79, yRK80, yRK81, and yRK83.
771
772 **Figure 4 Tel1-hy909 requires the MRX complex for the DNA damage response but not for**
773 **telomere elongation**
774
775 (A) Yeast dilution series of untreated cells or cells treated with 0.02% MMS for one hour. The
776 genotype is indicated to the left of the panels. To account for growth differences between the
777 genotypes different amounts of cells were collected for the initial dilution. 0.5 OD of cells were
778 collected for *WT* and *TEL1-hy909*, 1.5 OD of cells were collected for *mre11Δ,* and 8.0 OD of cells
779 were collected for *TEL1-hy909 mre11Δ*. Strains used in this assay were yRK114, yRK126,
780 yRK128, yRK104, yRK141, yRK92, yRK93, and yRK122. (B) Southern blot analysis of telomeres
781 from strains with the indicated genotype. Two independent, haploid segregants were assayed
782 for each genotype. Segregants are from JHUy816, yRK79, yRK80, yRK81, and yRK83. Cells
783 underwent minimal propagation before genomic DNA was prepared. (C) Southern blot analysis
784 of telomeres from strains with the indicated genotype. Two independent haploids segregants
785 were assayed for each genotype. Cells underwent minimal propagation before genomic DNA
786 was prepared. Segregants are from yRK5089, yRK5090, yRK5093, and yRK5094.
787 (D)-(E) CRISPR/Cas9 was used to knock-in the *rad50S* allele into a wild-type haploid strain
788 (yRK114). A transformant that was not edited at the *RAD50* locus but was transformed with the
789 Cas9 plasmid was used as a control and is referred to as *RAD50* (Figure 5D, lane 2). Both *RAD50*
790 and *rad50S* transformants were passaged on solid media for approximately 120 population

791 doublings (see 5D lanes 2-4, yRK2112-5, yRK2113-5, and yRK2116-5). *rad50S* or *RAD50* cells
792 were transformed to introduce *tel1Δ, mre11Δ* (Figure 5D lanes 5-10), or *TEL1-hy909* (Figure 5E
793 lanes 4-7). Cells were passaged on solid media for approximately 120 population doublings. The
794 strains used were yRK2118-5, yRK2120-5, yRK2121-5, yRK2122-5, yRK2123-5, yRK2124-5,
795 yRK2125-5, yRK2126-5, yRK2127-5, and yRK2128-5.
796
797 **Figure 5 Tel1 regulates telomere length in a pathway distinct from the DNA damage response**
798
799 Diagram demonstrating the distinctions between Tel1 pathways in the DNA damage response
800 and telomere length regulation. (A) The DNA damage response is most strongly regulated by
801 Mec1 and Rad53 as indicated with the bold arrows, although Tel1 signaling through Rad53 and
802 MRX plays a role. The MRX complex is both upstream and downstream of Tel1 in the DNA
803 damage response. (B) For telomere length regulation, Tel1 does not require MRX after
804 activation and Rad53 does not plan a role in the Tel1 telomere length regulation pathway. The
805 Tel1/MRX pathway plays the major role in telomere length compared to a minor role of
806 Mec1/Rad53 pathway.
807
808
809
810
811
812

943 **Literature Cited**

944

945 Alani, E., R. Padmore and N. Kleckner, 1990 Analysis of wild-type and rad50 mutants of
946 yeast suggests an intimate relationship between meiotic chromosome synapsis and
947 recombination. Cell 61**:** 419-436.

948 Albuquerque, C. P., M. B. Smolka, S. H. Payne, V. Bafna, J. Eng *et al.*, 2008 A multidimensional
949 chromatography technology for in-depth phosphoproteome analysis. Mol Cell
950 Proteomics 7**:** 1389-1396.

951 Anand, R., G. Memisoglu and J. Haber, 2017 Cas9-mediated gene editing in Saccharomyces
952 cerevisiae.

953 Armanios, M., and E. H. Blackburn, 2012 The telomere syndromes. Nature reviews. Genetics
954 13**:** 693-704.

955 Bahler, J., J. Q. Wu, M. S. Longtine, N. G. Shah, A. McKenzie, 3rd *et al.*, 1998 Heterologous
956 modules for efficient and versatile PCR-based gene targeting in
957 Schizosaccharomyces pombe. Yeast 14**:** 943-951.

958 Baldo, V., V. Testoni, G. Lucchini and M. P. Longhese, 2008 Dominant TEL1-hy mutations
959 compensate for Mec1 lack of functions in the DNA damage response. Mol Cell Biol
960 28**:** 358-375.

961 Bastos de Oliveira, F. M., D. Kim, J. R. Cussiol, J. Das, M. C. Jeong *et al.*, 2015
962 Phosphoproteomics reveals distinct modes of Mec1/ATR signaling during DNA
963 replication. Mol Cell 57**:** 1124-1132.

964 Becker, E., V. Meyer, H. Madaoui and R. Guerois, 2006 Detection of a tandem BRCT in Nbs1
965 and Xrs2 with functional implications in the DNA damage response. Bioinformatics
966 22**:** 1289-1292.
967 Bonetti, D., M. Martina, M. Clerici, G. Lucchini and M. P. Longhese, 2009 Multiple pathways
968 regulate 3' overhang generation at S. cerevisiae telomeres. Mol Cell 35**:** 70-81.
969 Boulton, S. J., and S. P. Jackson, 1996 Identification of a Saccharomyces cerevisiae Ku80
970 homologue: roles in DNA double strand break rejoining and in telomeric
971 maintenance. Nucleic Acids Res 24**:** 4639-4648.
972 Buis, J., Y. Wu, Y. Deng, J. Leddon, G. Westfield *et al.*, 2008 Mre11 nuclease activity has
973 essential roles in DNA repair and genomic stability distinct from ATM activation.
974 Cell 135**:** 85-96.
975 D'Amours, D., and S. P. Jackson, 2001 The yeast Xrs2 complex functions in S phase
976 checkpoint regulation. Genes Dev 15**:** 2238-2249.
977 de Lange, T., 2018 Shelterin-Mediated Telomere Protection. Annu Rev Genet 52**:** 223-247.
978 Di Domenico, E. G., E. Romano, P. Del Porto and F. Ascenzioni, 2014 Multifunctional role of
979 ATM/Tel1 kinase in genome stability: from the DNA damage response to telomere
980 maintenance. Biomed Res Int 2014**:** 787404.
981 Doench, J. G., N. Fusi, M. Sullender, M. Hegde, E. W. Vaimberg *et al.*, 2016 Optimized sgRNA
982 design to maximize activity and minimize off-target effects of CRISPR-Cas9. Nat
983 Biotechnol 34**:** 184-191.
984 Gibson, D. G., 2011 Enzymatic assembly of overlapping DNA fragments. Methods Enzymol
985 498**:** 349-361.

986 Goldstein, A. L., and J. H. McCusker, 1999 Three new dominant drug resistance cassettes for
987 gene disruption in Saccharomyces cerevisiae. Yeast 15**:** 1541-1553.
988 Green, M., and J. Sambrook, 2012 *Molecular Cloning: A Laboratory Manual*
989 Greider, C. W., 1999 Telomerase activation: one step on the road to cancer? Trends Genet
990 15**:** 109-112.
991 Greider, C. W., and E. H. Blackburn, 1987 The telomere terminal transferase of *Tetrahymena*
992 is a ribonucleoprotein enzyme with two kinds of primer specificity. Cell 51**:** 887-
993 898.
994 Gupta, A., S. Sharma, P. Reichenbach, L. Marjavaara, A. K. Nilsson *et al.*, 2013 Telomere
995 length homeostasis responds to changes in intracellular dNTP pools. Genetics 193**:**
996 1095-1105.
997 Hammond, P. W., and T. R. Cech, 1997 dGTP-dependent processivity and possible template
998 switching of euplotes telomerase [In Process Citation]. Nucleic Acids Res 25**:** 3698-
999 3704.
1000 Huang, M., Z. Zhou and S. J. Elledge, 1998 The DNA replication and damage checkpoint
1001 pathways induce transcription by inhibition of the Crt1 repressor. Cell 94**:** 595-605.
1002 Kaizer, H., C. J. Connelly, K. Bettridge, C. Viggiani and C. W. Greider, 2015 Regulation of
1003 Telomere Length Requires a Conserved N-Terminal Domain of Rif2 in
1004 Saccharomyces cerevisiae. Genetics 201**:** 573-586.
1005 Kim, S. T., D. S. Lim, C. E. Canman and M. B. Kastan, 1999 Substrate specificities and
1006 identification of putative substrates of ATM kinase family members. J Biol Chem
1007 274**:** 37538-37543.

1008 Kironmai, K. M., and K. Muniyappa, 1997 Alteration of telomeric sequences and senescence
1009 caused by mutations in RAD50 of *Saccharomyces cerevisiae*. Genes Cells 2**:** 443-455.
1010 Larrivee, M., C. LeBel and R. J. Wellinger, 2004 The generation of proper constitutive G-tails
1011 on yeast telomeres is dependent on the MRX complex. Genes Dev 18**:** 1391-1396.
1012 Lavin, M. F., S. Kozlov, M. Gatei and A. W. Kijas, 2015 ATM-Dependent Phosphorylation of
1013 All Three Members of the MRN Complex: From Sensor to Adaptor. Biomolecules 5**:**
1014 2877-2902.
1015 Lee, J. H., M. R. Mand, R. A. Deshpande, E. Kinoshita, S. H. Yang *et al.*, 2013 Ataxia
1016 telangiectasia-mutated (ATM) kinase activity is regulated by ATP-driven
1017 conformational changes in the Mre11/Rad50/Nbs1 (MRN) complex. J Biol Chem
1018 288**:** 12840-12851.
1019 Lee, S.-J., M. F. Schwartz, J. K. Duong and D. F. Stern, 2003 Rad53 Phosphorylation Site
1020 Clusters Are Important for Rad53 Regulation and Signaling. Molecular and Cellular
1021 Biology 23**:** 6300-6314.
1022 Lee, S. S., C. Bohrson, A. M. Pike, S. J. Wheelan and C. W. Greider, 2015 ATM Kinase Is
1023 Required for Telomere Elongation in Mouse and Human Cells. Cell Rep 13**:** 1623-
1024 1632.
1025 Lengsfeld, B. M., A. J. Rattray, V. Bhaskara, R. Ghirlando and T. T. Paull, 2007 Sae2 is an
1026 endonuclease that processes hairpin DNA cooperatively with the
1027 Mre11/Rad50/Xrs2 complex. Mol Cell 28**:** 638-651.
1028 Lingner, J., and T. R. Cech, 1998 Telomerase and chromosome end maintenance. Curr Opin
1029 Genet Dev 8**:** 226-232.

1030 Link, A. J., and J. LaBaer, 2011 Trichloroacetic acid (TCA) precipitation of proteins. Cold
1031 Spring Harb Protoc 2011**:** 993-994.
1032 Longhese, M. P., V. Paciotti, H. Neecke and G. Lucchini, 2000 Checkpoint Proteins Influence
1033 Telomeric Silencing and Length Maintenance in Budding Yeast. Genetics 155**:** 1577-
1034 1591.
1035 Ma, Y., and C. W. Greider, 2009 Kinase-independent functions of TEL1 in telomere
1036 maintenance. Mol Cell Biol 29**:** 5193-5202.
1037 Maicher, A., I. Gazy, S. Sharma, L. Marjavaara, G. Grinberg *et al.*, 2017 Rnr1, but not Rnr3,
1038 facilitates the sustained telomerase-dependent elongation of telomeres. PLoS Genet
1039 13**:** e1007082.
1040 Mallory, J. C., V. I. Bashkirov, K. M. Trujillo, J. A. Solinger, M. Dominska *et al.*, 2003 Amino
1041 acid changes in Xrs2p, Dun1p, and Rfa2p that remove the preferred targets of the
1042 ATM family of protein kinases do not affect DNA repair or telomere length in
1043 Saccharomyces cerevisiae. DNA Repair (Amst) 2**:** 1041-1064.
1044 Moore, J. K., and J. E. Haber, 1996 Cell cycle and genetic requirements of two pathways of
1045 nonhomologous end-joining repair of double-strand breaks in *Saccharomyces*
1046 *cerevisiae*. Mol Cell Biol 16**:** 2164-2173.
1047 Moreau, S., H. R. Ferguson and L. S. Symington, 1999 The nuclease activity of Mre11 is
1048 required for meiosis but not for mating type switching, end joiningor telomere
1049 maintenance. Mol. Cell Biol. in press.
1050 Moreau, S., E. A. Morgan and L. S. Symington, 2001 Overlapping functions of the
1051 Saccharomyces cerevisiae Mre11, Exo1 and Rad27 nucleases in DNA metabolism.
1052 Genetics 159**:** 1423-1433.

1053 Morrow, D. M., D. A. Tagle, Y. Shiloh, F. S. Collins and P. Hieter, 1995 TEL1, an S. cerevisiae
1054 homolog of the human gene mutated in ataxia telangiectasia, is functionally related
1055 to the yeast checkpoint gene MEC1. Cell 82**:** 831-840.
1056 Mumberg, D., R. Muller and M. Funk, 1995 Yeast vectors for the controlled expression of
1057 heterologous proteins in different genetic backgrounds. Gene 156**:** 119-122.
1058 Nakada, D., K. Matsumoto and K. Sugimoto, 2003a ATM-related Tel1 associates with
1059 double-strand breaks through an Xrs2-dependent mechanism. Genes Dev 17**:** 1957-
1060 1962.
1061 Nakada, D., T. Shimomura, K. Matsumoto and K. Sugimoto, 2003b The ATM-related Tel1
1062 protein of Saccharomyces cerevisiae controls a checkpoint response following
1063 phleomycin treatment. Nucleic Acids Res 31**:** 1715-1724.
1064 Norrander, J., T. Kempe and J. Messing, 1983 Construction of improved M13 vectors using
1065 oligodeoxynucleotide-directed mutagenesis. Gene 26**:** 101-106.
1066 Oh, J., and L. S. Symington, 2018 Role of the Mre11 Complex in Preserving Genome
1067 Integrity. Genes (Basel) 9.
1068 Paull, T. T., 2015 Mechanisms of ATM Activation. Annu Rev Biochem 84**:** 711-738.
1069 Paull, T. T., 2018 20 Years of Mre11 Biology: No End in Sight. Molecular Cell 71**:** 419-427.
1070 Pfeiffer, V., and J. Lingner, 2013 Replication of telomeres and the regulation of telomerase.
1071 Cold Spring Harb Perspect Biol 5**:** a010405.
1072 Ralser, M., H. Kuhl, M. Ralser, M. Werber, H. Lehrach *et al.*, 2012 The Saccharomyces
1073 cerevisiae W303-K6001 cross-platform genome sequence: insights into ancestry
1074 and physiology of a laboratory mutt. Open Biol 2**:** 120093.

1075 Ritchie, K. B., J. C. Mallory and T. D. Petes, 1999 Interactions of TLC1 (which encodes the
1076 RNA subunit of telomerase), TEL1, and MEC1 in regulating telomere length in the
1077 yeast Saccharomyces cerevisiae. Mol Cell Biol 19**:** 6065-6075.
1078 Sanchez, Y., B. A. Desany, W. J. Jones, Q. Liu, B. Wang *et al.*, 1996 Regulation of RAD53 by the
1079 ATM-like kinases MEC1 and TEL1 in yeast cell cycle checkpoint pathways. Science
1080 271**:** 357-360.
1081 Shima, H., M. Suzuki and M. Shinohara, 2005 Isolation and characterization of novel xrs2
1082 mutations in Saccharomyces cerevisiae. Genetics 170**:** 71-85.
1083 Sikorski, R. S., and J. D. Boeke, 1991 In vitro mutagenesis and plasmid shuffling: from
1084 cloned gene to mutant yeast. Methods Enzymol 194**:** 302-318.
1085 Sikorski, R. S., and P. Hieter, 1989 A system of shuttle vectors and yeast host strains
1086 designed for efficient manipulation of DNA in Saccharomyces cerevisiae. Genetics
1087 122**:** 19-27.
1088 Smolka, M. B., C. P. Albuquerque, S. H. Chen and H. Zhou, 2007 Proteome-wide identification
1089 of in vivo targets of DNA damage checkpoint kinases. Proc Natl Acad Sci U S A 104**:**
1090 10364-10369.
1091 Stanley, S. E., and M. Armanios, 2015 The short and long telomere syndromes: paired
1092 paradigms for molecular medicine. Curr Opin Genet Dev 33**:** 1-9.
1093 Tong, A. S., J. L. Stern, A. Sfeir, M. Kartawinata, T. de Lange *et al.*, 2015 ATM and ATR
1094 Signaling Regulate the Recruitment of Human Telomerase to Telomeres. Cell Rep
1095 13**:** 1633-1646.

1096 Tsukamoto, Y., A. K. Taggart and V. A. Zakian, 2001 The role of the Mre11-Rad50-Xrs2
1097 complex in telomerase- mediated lengthening of Saccharomyces cerevisiae
1098 telomeres. Curr Biol 11**:** 1328-1335.
1099 Usui, T., H. Ogawa and J. H. Petrini, 2001 A DNA damage response pathway controlled by
1100 Tel1 and the Mre11 complex. Mol Cell 7**:** 1255-1266.
1101 Viscardi, V., D. Bonetti, H. Cartagena-Lirola, G. Lucchini and M. P. Longhese, 2007 MRX-
1102 dependent DNA damage response to short telomeres. Mol Biol Cell 18**:** 3047-3058.
1103 Winzeler, E. A., D. D. Shoemaker, A. Astromoff, H. Liang, K. Anderson *et al.*, 1999 Functional
1104 characterization of the S. cerevisiae genome by gene deletion and parallel analysis.
1105 Science 285**:** 901-906.
1106 Zhao, X., E. G. Muller and R. Rothstein, 1998 A suppressor of two essential checkpoint genes
1107 identifies a novel protein that negatively affects dNTP pools. Mol Cell 2**:** 329-340.
1108

Figure 1

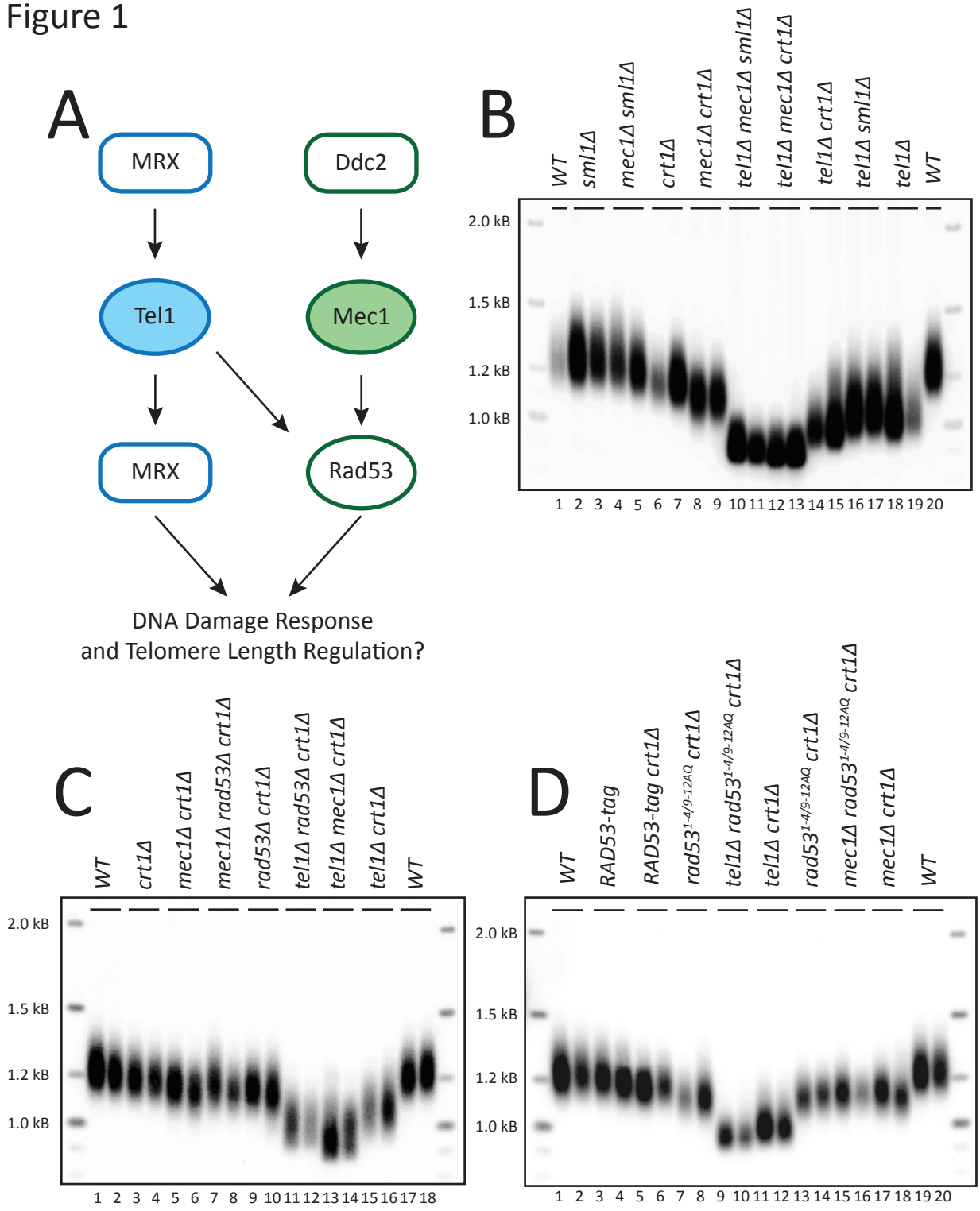

Figure 2

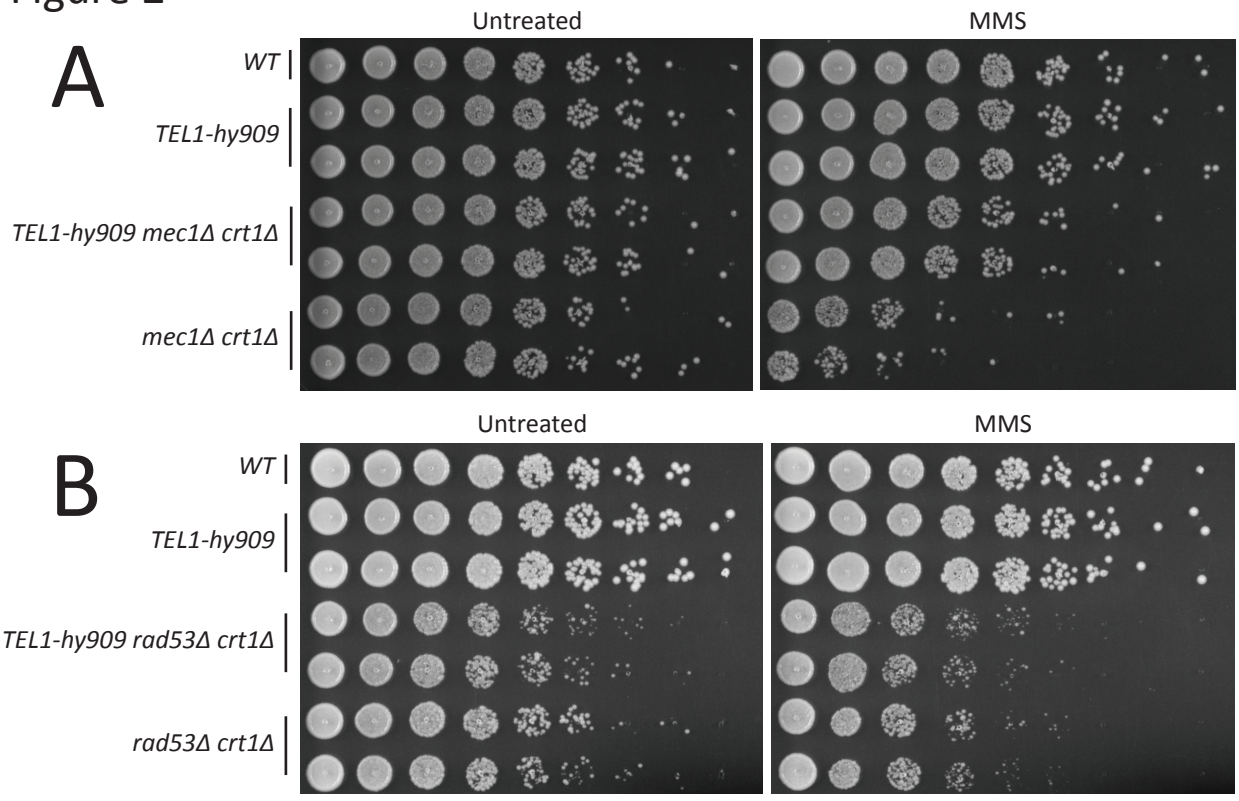

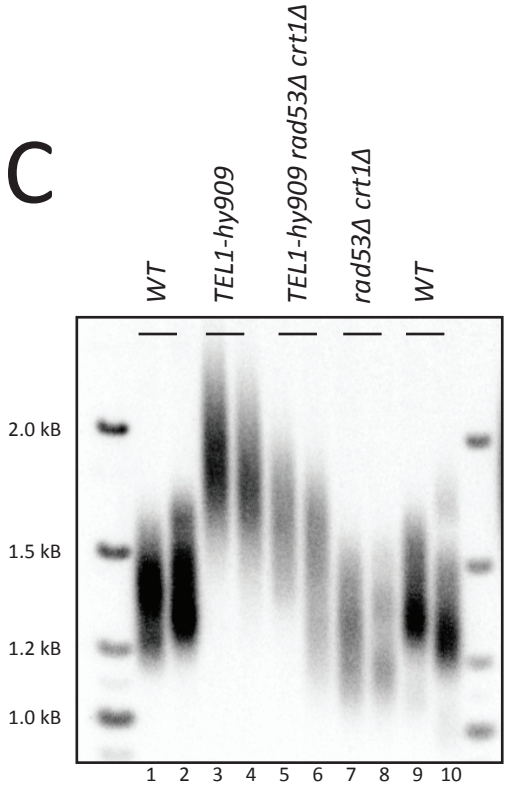

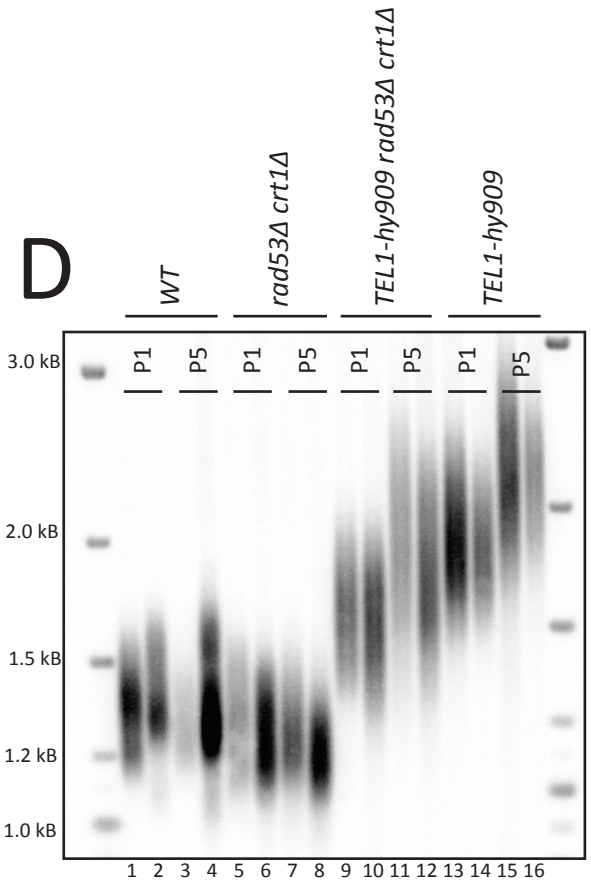

Figure 3

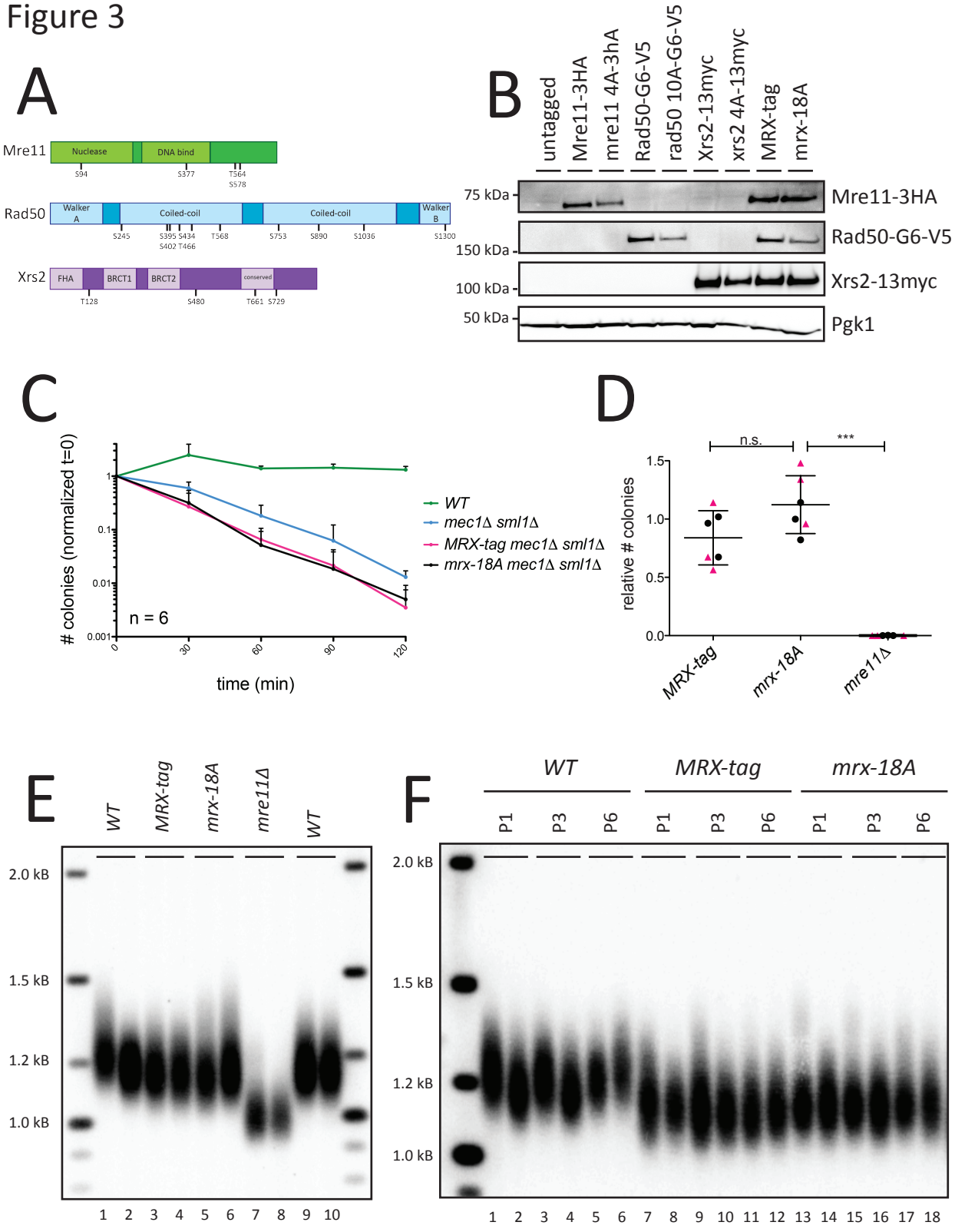

Figure 4

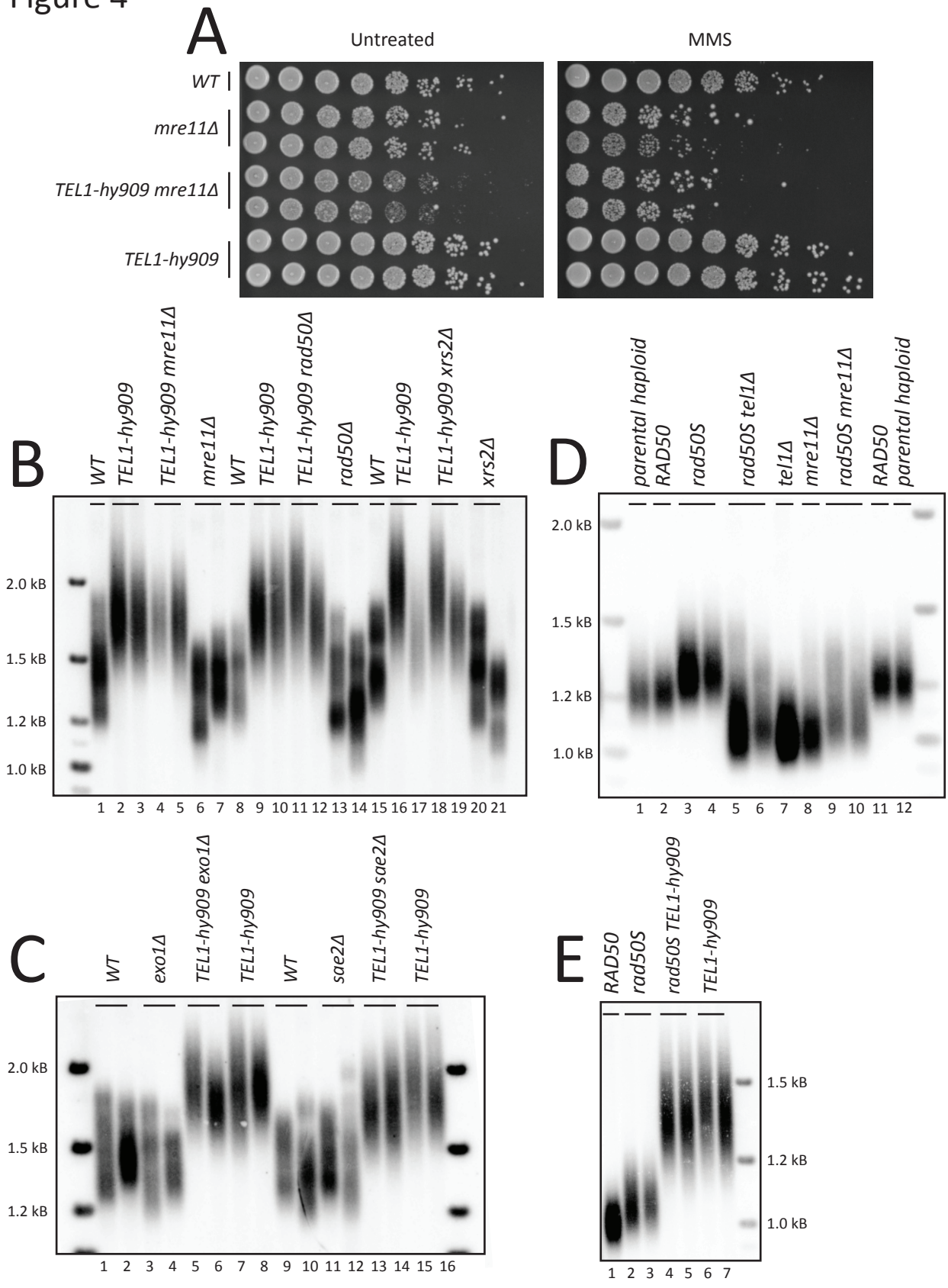

Figure 5